Ceramics International 49 (2023) 1888–1895

Contents lists available at ScienceDirect

Ceramics International

journal homepage: www.elsevier.com/locate/ceramint

Magnetocrystalline anisotropy study of Co-substituted M-type strontium hexaferrite single crystals

Ruoshui Liu [a,b,c,**], Lichen Wang [d,e], Xiang Yu [b,c], Zhiyi Xu [b,c], Huayang Gong [b], Tongyun Zhao [b,c], Fengxia Hu [c], Baogen Shen [a,b,c,d,e,*]

[a] School of Rare Earths, University of Science and Technology of China, Hefei, Anhui, 230026, China
[b] Ganjiang Innovation Academy, Chinese Academy of Sciences, Ganzhou, Jiangxi, 341119, China
[c] Beijing National Laboratory for Condensed Matter Physics, Institute of Physics, Chinese Academy of Sciences, Beijing, 100190, China
[d] Ningbo Institute of Materials Technology & Engineering, Chinses Academy of Sciences, Ningbo, Zhejiang, 315201, China
[e] Innovation Center for Applied Magnetics of Zhejiang Province, Ningbo, Zhejiang, 315201, China

ARTICLE INFO

Keywords:
Strontium hexaferrite
Single crystal
Magnetic anisotropy
Co-substitution

ABSTRACT

The study on the magnetocrystalline anisotropy (MA) of La–Co co-substituted strontium hexaferrite (La–Co SrM) shows a joint effect of Fe^{2+} and Co^{2+} ions in the enhancement of MA. Since the role of Fe^{2+} single ion has been studied with La-substituted strontium ferrite, in this work, Co-substituted strontium hexaferrite $SrFe_{12-x}Co_xO_{19}$ (Co-SrM) single crystals were successfully grown for $0 \leq x \leq 0.31$ by the Na_2CO_3 flux method to elucidate the anisotropy of Co^{2+} single ions. Co-substitution in this preparation condition has a limit solubility of 0.31 and enhances uniaxial magnetic anisotropy field H_A by 19% for $0.03 = x \leq 0.11$, with a mere loss of 7% of saturation magnetization M_S at 5 K. The enhanced H_A of Co-SrM is reported for the first time, even higher than that of La–Co SrM, which is suitable to be used as permanent magnets in this concentration range. But with the further substitution of Co, the planar anisotropy of $x = 0.31$ was observed at 5 K. The potential nonlinear magnetic structure of Co-SrM remains to be discovered for magnetoelectric effects. This work is also of great significance as a complement to the magnetocrystalline anisotropy study of La–Co SrM.

1. Introduction

Magnetoplumbite-type (M-type) strontium hexaferrite like $SrFe_{12}O_{19}$ (SrM), permanent magnets have increased progressive attention due to the large uniaxial magnetic crystalline anisotropy, cost-effective and chemical stability [1–4]. Therefore, many efforts have been made to optimize the permanent properties by chemical modification. Especially, the 20% enhancement in the coercivity H_{cJ} can be obtained by simultaneous substitution of La and Co in SrM [5,6], and has been directly commercialized. At the same time, the residual angular momentum of Co^{2+} ($3d^7$) is responsible for the large magnetocrystalline anisotropy (MA) and the optimized permanent performance. Although many efforts have been devoted to clarifying the correlation between the occupation sites of Co substitution and enhanced MA, to date, the underlying mechanism is not clear since Co site preference has always been a controversial issue [7–16]. The complicated crystal structure and limited Co solubility make it difficult to identify the Co occupation sites, furthermore, polycrystalline samples also bring challenges to the experimental analysis due to the complex local structures and defects. Thus, high-quality single crystals are essential to study the critical role of Co substitution in the enhanced MA.

Systemic research on single crystals $AB_{12}O_{19}$ (A = Sr, Ca, Na, etc; B = Fe, Co) has been adopted by researchers worldwide in recent years. Shimoda et al. [17] have studied MA of La and La–Co substituted SrM single crystals prepared by the Na_2O flux method. For $Sr_{1-x}La_xFe_{12}O_{19}$, the dilution of magnetic uniaxial anisotropy with increasing x within $x \leq 0.5$ is related to the appearance of Fe^{2+} due to the charge balance. For $Sr_{1-x}La_xFe_{12-y}Co_yO_{19}$ compounds, the uniaxial anisotropy is enhanced, resulting from the Co substitution instead of Fe^{2+}. Furthermore, Ueda et al. prepared single crystals $Sr_{1-x}La_xFe_{12-y}Co_yO_{19}$ ($x = y$ for $x \leq 0.4$, $y = 0.4$ for $x \geq 0.4$) by traveling solvent floating zone (TSFZ) technique [18]. The spin-orbit coupling of substituted Co^{2+} ions is mainly responsible for the enhancement of uniaxial anisotropy for $x \leq 0.4$, while the produced Fe^{2+} further enhances the uniaxial anisotropy for $x \geq 0.4$. And

* Corresponding author. School of Rare Earths, University of Science and Technology of China, Hefei, Anhui, 230026, China.
** Corresponding author. School of Rare Earths, University of Science and Technology of China, Hefei, Anhui, 230026, China.
E-mail addresses: liuruoshui123@iphy.ac.cn (R. Liu), shenbg@iphy.ac.cn (B. Shen).

https://doi.org/10.1016/j.ceramint.2022.09.153
Received 22 July 2022; Received in revised form 1 September 2022; Accepted 12 September 2022
Available online 16 September 2022

then Waki et al. continued to study this problem in-depth and prepared single crystals Ca–La–Co and Na–La–Co magnets to compare the Co-substituted M-type ferrites with different non-magnetic *A* cations and to clarify the mechanism of the *A* cations affect in the MA [19,20]. Meanwhile, massive works have focused on the effect of Co^{2+} co-substitution with another tetravalent ion [21–23], while the effect of a single *B* cation, especially Co^{2+}, on the MA of SrM has been somehow neglected.

On the other hand, Co^{2+} substitution is important in manipulating easy-axis in hexaferrite and even in spinel ferrite [24–26]; predominantly planer anisotropy has been observed for Co–Ti co-substituted M-type ferrite and other types of hexaferrite, such as Y-type $SrFe_{12}Co_2O_{22}$ [27] and X-type $Sr_2Fe_{28}Co_2O_{46}$ [28,29]. Furthermore, Co-substituted M-type hexaferrite polycrystalline samples were studied as microwave materials as well as magnetic and magneto-optical recording media [30–38], while the magnetic properties showed great variation with different preparation methods. Nevertheless, Vinnik et al. prepared Co-substituted BaM single crystals by Na_2CO_3 flux and magnetic properties were measured by powder sample [39]. However, it is misty to attribute the reduced H_{cJ} of single-crystal powder to the decrease in MA, because H_{cJ} is a structure-sensitive parameter and the H_{cJ} of single crystals is close to zero due to the easily movable domain walls [40], while MA is an inherent property of materials. In addition, Dixit et al. investigated the effect of Co-substitution at the Fe sites on the magnetic properties of SrM by using the first-principles method based on density functional theory [41]. The enhancement of anisotropic field H_A by 17.1% in the Co substitution showed a contradiction between the experimental and calculated results.

Considering the enhanced MA of La–Co co-substituted SrM is influenced by the joint Co^{2+} and Fe^{2+}, the effect of single ion Fe^{2+} has been studied in detail through La-SrM [42], while the effect of single ion Co^{2+} remains dimness yet. This work reveals the effect of the Co-substitution on MA through the macroscopic magnetic and structural analysis in $SrFe_{1-x}Co_xO_{19}$ (Co-SrM, $0 \leq x \leq 0.31$) single crystals. Interestingly, enhanced H_A was obtained at a relatively slight Co substitution concentration ($0.03 < x \leq 0.11$), and even higher than La–Co SrM with the same Co concentration, which is because of the occupation of the 12*k* site by Co ions to compensate for the negative effect of this site on MA. The high permanent magnetic performance in this range is beneficial for practical applications. Besides, with a further increase in Co-substitution, the uniaxial anisotropy becomes planar anisotropy which the 12*k* and 2*a* sites prefer and results in a decrease in H_A. It can be speculated from this study that, Co only contributes to uniaxial anisotropy when co-substituted with the rare earth ion La, otherwise Co favors planar anisotropy when substituted alone or with other ions, which is essentially caused by different occupancies.

2. Experiments

The parent and Co substituted M-type strontium hexaferrite single crystals were grown by the Na_2CO_3 flux method. $SrCO_3$ (99.95%), Fe_2O_3 (99.99%), Co_3O_4 (99.99%), and Na_2CO_3 (99.9%) were weighed and mixed well by a planet ball mill for 12 h. All raw materials were proportioned according to nominal substitutions shown in Table 1, where the mole ratio of Na/Sr is 4.995. And then, the initial mixture was filled into a 30 mL platinum crucible and heated in a furnace under an ambient atmosphere. The furnace was maintained at 1260 °C for 3 h followed by cooling with a rate of 2.5 °C/h to 900 °C and naturally cooled down to room temperature. After that, these crystals were separated from the solidified melt by leaching in hot hydrochloric acid and cut typically into rectangular with a typical size of 3×3×1 mm^3 to reduce the demagnetization factor, which was calculated according to a reported method [43]. To confirm a single M-type phase of the samples and estimate lattice parameters, part of these crystals were crushed into powder for X-ray diffractometer (XRD, Rigaku D/Max-2400) measurement. The concentrations of the elements were measured by inductively coupled plasma atomic emission spectrometry (ICP-AES, IRIS Intrepid II XDL). The Curie temperatures were determined using a differential scanning calorimeter (DSC, Netzsch STA-449). The magnetization measurement is performed on the vibrating sample magnetometer (SQUID-SVM, Quantum Design) in the temperate range of 5–300 K and fields up to 50 kOe. After eliminating the shape anisotropy of samples by calculating the demagnetization factors, the hard-axis ($H \perp c$) and easy-axis ($H \| c$) magnetization curves were normalized to get their saturation magnetization M_S and magnetocrystalline anisotropy (MA). The anisotropic field H_A is usually defined as the field where the hard magnetization saturates, which is evaluated as an indicator of MA. But the hard magnetization curves of ion-substituted hexaferrite are not linear and cannot be estimated by the singular point detection (SPD) method [44]. Thus, the formula $H_A = 2K_1/M_S$ was adopted to discuss the MA, where K_1 is the first anisotropy constant, estimated by the area surrounded by easy- and hard-magnetization curves.

3. Results and discussion

The schematic crystal structure of M-type strontium hexaferrite (SrM) is depicted in Fig. 1(a). It is obvious that the SrM crystallized in hexagonal ferrite can be considered as an alternating stacking of the Sr-containing hexagonal R block and the spinel S block along the *c*-axis. The block turned 180° around the hexagonal *c*-axis marked out by symbol *. Five inequivalent Fe sites with three octahedral sites (2*a*, 4f_2, 12*k*), one bipyramidal site (2*b*), and one tetrahedral site (4f_1) in the unit cell are shown in Fig. 1(a). The superexchange interaction between oxygen and iron atoms split the magnetic structure to the majority spin up at 2*a*, 2*b* and 12*k*, and the minority spin down at 4f_1 and 4f_2 sites along the *c*-axis, resulting in a ferrimagnetic structure with 20 μ_B per formula unit (f.u.). Fig. 1(b) shows the obtained regular hexagonal shapes single crystal of SrM with general sizes up to 5 mm. Room-temperature X-ray powder diffraction patterns were collected on pulverized single crystals as shown in Fig. 1(c), and the lattice parameters obtained by Rietveld refinement were shown in Table 1. All peaks can be indexed as the M-type hexaferrite crystallized in a hexagonal unit cell with space group $P6_3/mmc$. And the X-ray diffraction pattern for SrM single crystal is also shown in Fig. 1(c), with diffraction peaks only indexed as the (00*l*)

Table 1
Chemical composition, lattice parameters, magnetic properties, and Curie temperature for $SrFe_{12-x}Co_xO_{19}$ single crystals.

Sample	x[a]	a	c	V	M_S (μ_B/f.u.)		H_A (kOe)		T_C
		Å	Å	Å^3	5 K	300 K	5 K	300 K	K
SrM	0 [0]	5.8817(1)	23.0336(7)	689.10(5)	19.97(3)	14.09(1)	17.43	18.50	742.23
$Co_{0.03}$	0.0316 [0.1]	5.8859(3)	23.0429(4)	689.45(4)	18.86(4)	13.57(6)	18.39	18.98	736.52
$Co_{0.05}$	0.0542 [0.2]	5.8878(5)	23.0429(1)	689.46(4)	18.48(5)	12.97(1)	20.76	19.90	730.43
$Co_{0.11}$	0.1059 [0.4]	5.8884(3)	23.0330(2)	688.37(3)	18.54(2)	13.29(5)	20.32	20.98	726.05
$Co_{0.15}$	0.1521 [0.5]	5.8797(4)	23.0257(6)	687.55(8)	17.49(1)	12.54(5)	18.01	18.72	723.15
$Co_{0.20}$	0.1974 [1.0]	5.8778(4)	23.0214(5)	687.16(5)	17.22(1)	12.35(3)	16.12	15.80	721.68
$Co_{0.25}$	0.2497 [1.2]	5.8764(2)	23.0197(1)	687.11(7)	16.60(2)	11.90(3)	14.10	14.85	721.14
$Co_{0.31}$	0.3109 [1.5]	5.8680(3)	22.9826(2)	687.01(1)	16.72(3)	11.42(1)	5.36	10.18	720.25

[a] Values in [ ] means nominal compositions.

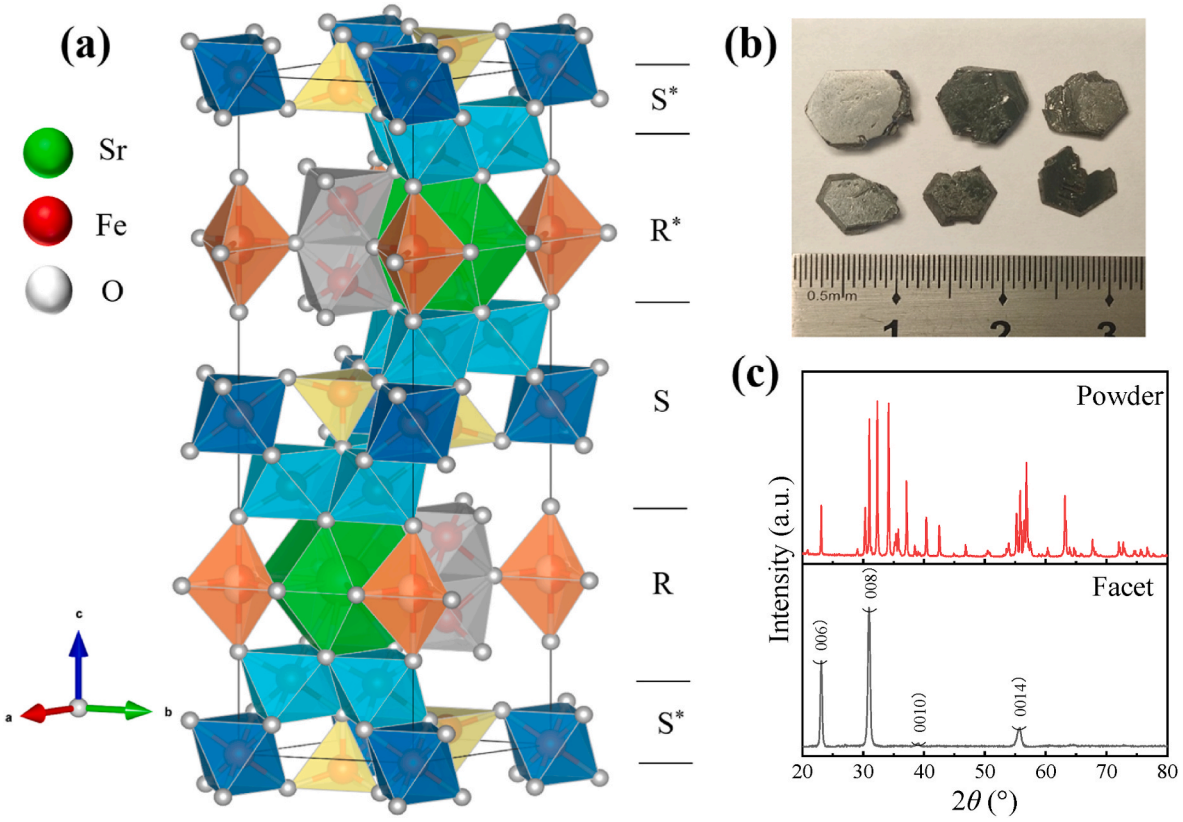

Fig. 1. (a) Schematic crystal structure, (b) the obtained single crystals of $SrFe_{12}O_{19}$, and (c) the XRD patterns of powder and the surface for $SrFe_{12}O_{19}$ single crystal.

plane, indicating the highly-orientation in the samples.

The Co-substituted single crystals $SrFe_{12-x}Co_xO_{19}$ (Co-SrM) were grown by using the Na_2CO_3 flux method. The Co actual concentration is determined by ICP measurements and listed in Table 1, accounting for merely 18% of the nominal amount on average. For simple description, $SrFe_{11.97}Co_{0.03}O_{19}$, can be denoted as $Co_{0.03}$, and the rest can be followed by analogy. As detected by XRD, Co-SrM single crystals without any impurity were obtained in the range of x values from 0.03 to 0.31, the solubility limit of 0.31 is consistent with the previous reports [33, 39]. With the increase of Co substitution, the variation between the actual and nominal concentration becomes larger due to the second phase such as $CoFe_2O_4$. The limited solubility in M-type hexaferrite is

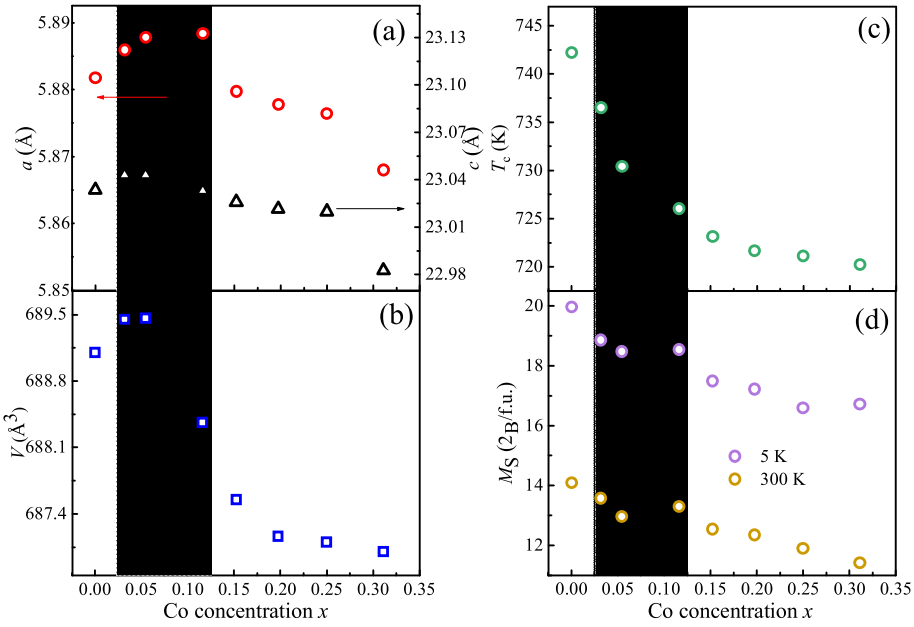

Fig. 2. Co concentration x dependencies of (a) lattice parameters a and c, (b) cell volume V, (c) Curie temperature T_C, and (d) saturation magnetization M_S at 5 K and 300 K. The abnormal changes in cell parameters were marked out by the green rectangle. (For interpretation of the references to colour in this figure legend, the reader is referred to the Web version of this article.)

due to the charge compensation mechanism since Co is divalent while Fe is trivalent. For simple aliovalent substitution the homogeneity ranges, i.e., x typically remains small. In the case of complete substitution with divalent Co ions, the charge balance causes vacancies in the oxide substructure, which may preferentially occur on one or several of five different crystallographic sites [35].

The lattice parameters a, c, and unit cell volume V of Co-SrM are shown in Fig. 2(a)-(b). At very low concentrations for Co, some increases were observed in the unit cell parameters compared to pure SrM, which is because the radius of Co^{2+} ion (0.74 Å) is larger than that of Fe^{3+} ion (0.67 Å). Nevertheless, with the higher increase of Co concentration, a monotonical decrease of lattice parameters occurred. It may be postulated that some oxygen vacancies must exist to maintain the electroneutrality of the structure when the Fe^{3+} ions are replaced by divalent ions. Consequently, accurate thermogravimetric analysis (TGA) was carried out in an attempt to confirm their existence in the Co-SrM. The samples were measured under oxygen atmosphere to examine oxidation of Co^{2+} ions, using temperature of 10 °C/min from 20 to 1200 °C. The TGA results of all samples, except pure SrM, exhibited varying degrees of weight gain at the end of heating as shown in Fig. 3. The consequences of the weight gain in terms of stoichiometry are shown in Table 2. The calculated oxygen vacancies δ are similar to the theoretical values obtained from the chemical formula, proving that the weight gain was due to the filling the oxygen vacancies and that the substituted Co ions in these samples are divalent Co^{2+} and not Co^{3+}, otherwise the TG curves would not have such a significant weight increase. It is certainly the above results do not completely exclude the presence of Co^{3+}, but the amount of Co^{3+} is very tiny even when exit in ferrites [13] under the current experimental conditions and can be further confirmed by nuclear magnetic resonance in the future.

Besides, the Curie temperature T_C as a function of Co concentration is exhibited in Fig. 2(c). Similar to the ion-substitution hexaferrite magnets, T_C monotonically decreases with Co concentration due to the weakening of Fe–*O*–Fe interactions by Co substitution. Saturation magnetizations M_S were obtained as shown in Fig. 2(d). In general, M_S decreases with the increase of Co concentration at all temperature, and notably, M_S keep a relatively high value with slight Co concentration, which is consistent with the green rectangle marked out. To date, the occupied sites of Co-substituted Sr hexaferrite are not clear. Some studies suggest that Co ions occupy $4f_2$ and $2b$ sites [37,45], but this is not accurate because the single Co-substituted ferrite is not the same as those with La–Co or Co–Ti substitution, and the presence of other ions may cause Co to occupy specific sites. It was been calculated that Co preferentially occupied $12k$ and $2a$ by first principles [41]. To sum up,

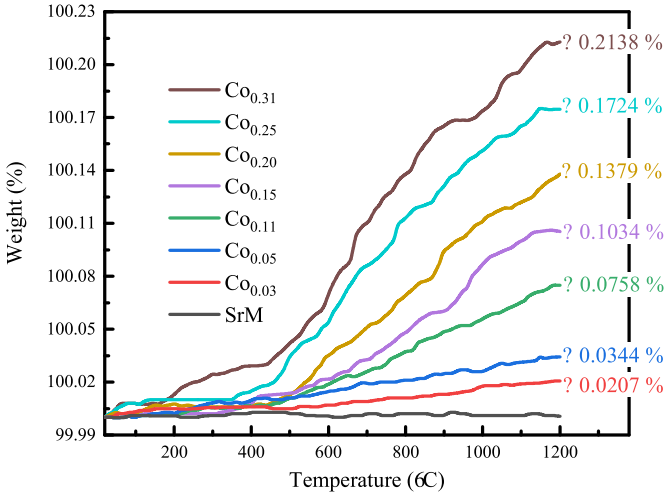

Fig. 3. TG curves of $SrFe_{12-x}Co_xO_{12}$ single crystals from 20 to 1200 °C at 10 °C/min under oxygen atmosphere.

Table 2
TGA of $SrFe_{12-x}Co_xO_{19-\delta}$ samples.

Samples	Calculated weight increase (%)	Calculated oxygen vacancies (%)	Calculated δ	Theoretical values of δ
SrM	0	0	0	0
$Co_{0.03}$	0.0207	0.0722	0.0137	0.015
$Co_{0.05}$	0.0344	0.1202	0.0228	0.025
$Co_{0.11}$	0.0758	0.2645	0.0502	0.055
$Co_{0.15}$	0.1034	0.3606	0.0685	0.075
$Co_{0.20}$	0.1379	0.4807	0.0913	0.100
$Co_{0.25}$	0.1724	0.6001	0.1141	0.125
$Co_{0.31}$	0.2138	0.7448	0.1414	0.155

the decreased M_S is because Co^{2+} mainly occupies the spin upward sites and the magnetic moment of Co^{2+} (3 μ_B) is less than Fe^{3+} (5 μ_B), but the occupancy may change with increasing concentration.

For permanent magnets, the coercivity is closely related to magnetocrystalline anisotropy (MA). The anisotropic field H_A can visually characterize the strength of uniaxial anisotropy and can be obtained by using the magnetization curves of the magnetic field H along with the different directions in the single crystals. In this context, the magnetization curves of the $SrFe_{12-x}Co_xO_{19}$ ($0 \le x \le 0.31$) with H parallel and perpendicular to the c-axis at 5 K are shown in Fig. 4(a). Obviously, all Co-SrM single crystals exhibit uniaxial MA similar to SrM at 5 K, except for $Co_{0.31}$ where the easy magnetization axis is within the *ab*-plane due to the easier magnetization of the hard-axis than the easy-axis at low fields. As Co concentration x increases, the H at which the hard-axis magnetization curves reach saturation increases first and then decreases, indicating that the non-monotonic variation of the MA of Co^{2+} in the concentration range of $0 = x \le 0.31$. In previous reports, the increased anisotropy of La–Co SrM resulted from the effect of Co^{2+} [17,18], and the MA effect of Fe^{2+} ion on La-SrM is concentration- and temperature-dependent [42]. In this work, the slight Co single ion exhibit an optimized effect on the MA of Co-SrM, while the heavy Co single ion will dilute the MA, which will be discussed from concentration and temperature.

The isothermal magnetization curves of $Co_{0.31}$ parallel and perpendicular to the c-axis at 5 K and 300 K are shown in Fig. 4(b). Compared with the c-axis, it is easier to be magnetized under a low magnetic field in the *ab*-plane, showing the characteristics of planar anisotropy at 5 K marked in the red rectangle. Moreover, a spin reorientation transition from an easy plane to an easy axis state with the temperature increasing was verified by the temperature-dependent magnetization curves in two directions of $Co_{0.31}$, as shown in the inset of Fig. 4(b). The temperature of this transition T_{SR} was approximately 59 K by differentiating the curve in the direction of $H \perp c$. Such anomalies will make the estimated H_A extremely small. As the temperature rises to 300 K, $Co_{0.31}$ exhibits typical uniaxial anisotropy but the nonlinear hard-axis magnetization curve also shows the presence of a nonlinear magnetic structure. Actually, A. M. Balbashov et al. [46] have prepared $SrCo_xMg_{0.125x}Fe_{12-1.125x}O_{19}$ single crystal with Co concentration of 0.8 by floating zone method, showing the main phase of this sample is W-type instead of M-type. Therefore, a complete planar MA was introduced to this sample in all temperature ranges. Similarly, J. Kreisel et al. [47] found that the MA of Co–Ti BaM transformed from uniaxial into planar with the increases of Co–Ti concentration due to the conical magnetic structure. The reason for this transition is that Co^{2+} occupies the $12k$ and $2a$ octahedral sites, while the tetrahedral sites have a strong noncubic (triangular) component in the nearest neighbor crystalline field [48]. Thus, it can be predicted that a further increase in Co substitution for $x > 0.31$ leads to the change from uniaxial to planar anisotropy and increases the tendency of the conical magnetic structure, resulting in magnetoelectric effects similar to those of $BaFe_{12-x}Co_xTi_xO_{19}$ [49] and $SrFe_{1-x}Sc_xO_{19}$ [50] systems. Hence Co-substituted M-type ferrite can be used to reduce the loss at high frequencies whilst enhancing the

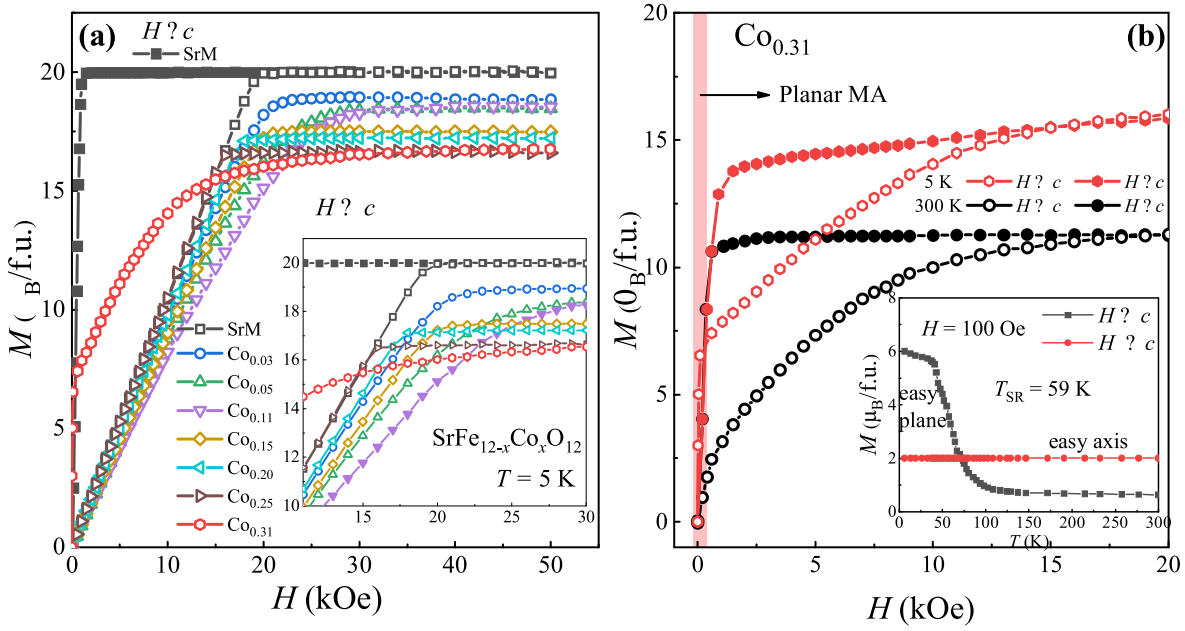

Fig. 4. (a) Easy- ($H\|c$) and hard-axis ($H\perp c$) magnetization curves of $SrFe_{12-x}Co_xO_{12}$ single crystals. The field has been corrected for the demagnetizing field by taking account of the sample shape [43]. The easy-axis curve is shown for only $SrFe_{12}O_{19}$. The inset shows the magnified view at 10–30 kOe. (b) Magnetization curves of $Co_{0.31}$ measured parallel and perpendicular to the *c*-axis at 5 K (red) and 300 K (black) with the inset of temperature dependence in both directions under 100 Oe. The planar anisotropy characteristic of $Co_{0.31}$ at 5 K is marked out by the red rectangle. (For interpretation of the references to colour in this figure legend, the reader is referred to the Web version of this article.)

permeability of microwave material [32,34,51].

Fig. 5(a) shows the magnetic anisotropy H_A plotted against Co concentration x at 5 K. As seen previously, Co^{2+} promotes the MA when $x \leq 0.15$, which is consistent with the calculations in the literature [41]. However, when $0.15 < x \leq 0.31$, Co^{2+} shows a negative effect on MA, which can be supported by most experimental results [34,48,51–53]. There would be two possible explanations, "site selectivity" and "local strain". On one hand, the anisotropy constants for each site of Fe^{3+} ions in M-type ferrite have been calculated and it was found that only the 12*k* site hurts the anisotropy [54], so Co^{2+} occupying the 12*k* site can compensate for part of the negative effect. But when concentration becomes higher, despite the large orbital moments of Co^{2+} ions at 12*k* and 2*a* sites, they may act negatively on MA, preferring planar or cone MA instead [55]. On the other hand, the magnitude of the Co orbital moment, as an origin of the anisotropy, is expected to correlate with the local strain of the coordination polyhedron [14]. For example, Ca–La–Co system with small *c*/*a* ratios exhibited larger MA than Na–La–Co system when the Co concentration is low [56]. As the inset of Fig. 5(a) shows, the *c*/*a* ratios of Co-SrM single crystals decrease when $x \leq 0.15$, which implies the coordination polyhedral is shrunk along with *c*, resulting in an enhancement of the uniaxial MA. When $0.15 < x \leq 0.31$, the *c*/*a* ratio increases and becomes larger, and different extent of the local strain can

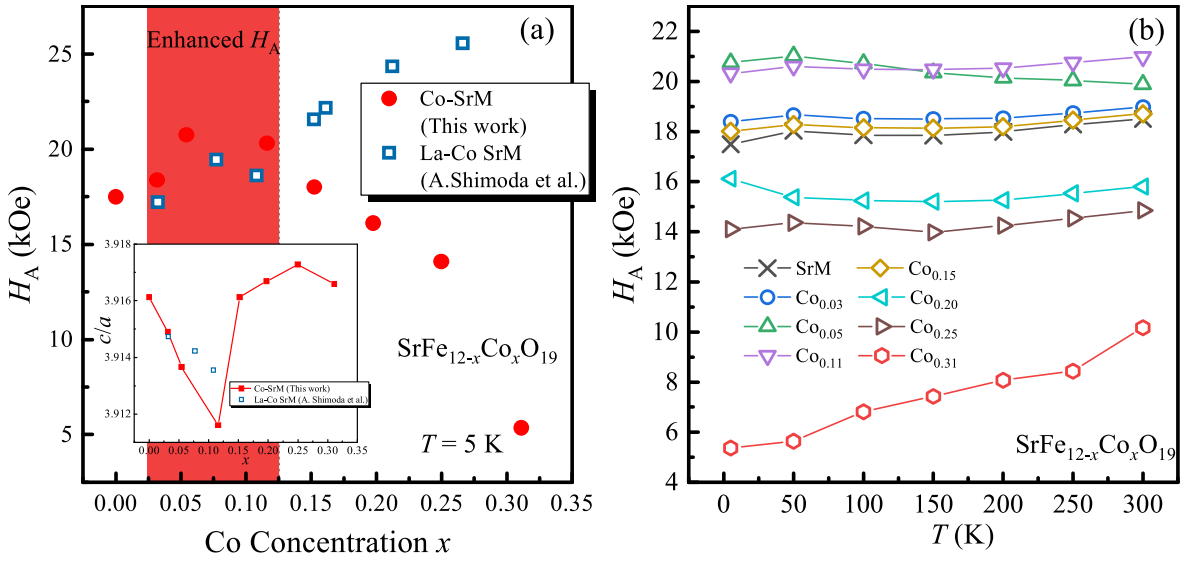

Fig. 5. (a)Magnetic anisotropy field, H_A, at 5 K for $SrFe_{12-x}Co_xO_{19}$ (the red circles) plotted against Co concentration *x*. Data of the La–Co SrM single crystals [17] (the blue squares) are also plotted. The highlighted area shows that the H_A of Co SrM is higher than that of La–Co SrM in this Co concentration range. The inset is the lattice parameter *c*/*a* ratio of Co SrM (the red dotted line) and La–Co SrM [17] (the blue squares) against *x*. (b) The temperature dependence of H_A for all samples. (For interpretation of the references to colour in this figure legend, the reader is referred to the Web version of this article.)

be responsible for the difference in anisotropy. Further work is necessary to confirm the speculation after the determination of Co^{2+} occupancy in Co-SrM.

It is worth mentioning in Fig. 5(a) that when $x \leq 0.15$, the H_A of Co-SrM is larger than that of La–Co SrM [17] at 5 K as the same Co substitution concentration due to the smaller c/a value of Co-SrM than that of La–Co SrM [52,53]. To our knowledge, the enhanced H_A of Co-SrM in this Co concentration range has not been reported before, with H_A increasing by 19% and M_S only losing 7% at 5 K for $Co_{0.05}$ compared to that of SrM. However, with the further increase of x, the H_A of La–Co SrM increases monotonically while that of Co-SrM keeps decreasing. It can be concluded that the Co^{2+} single ion inhibits the uniaxial anisotropy of M-type ferrite when $0.15 < x \leq 0.31$. As mentioned earlier, Co-substitution with other ions reduces the magnetic anisotropy [57–60], but increases with rare-earth ions [61,62]. It is also known that Fe^{2+} single ion has a negative effect on H_A at low concentrations [63]. Therefore, the enhancement of MA in La–Co SrM must be due to the joint influence of Co^{2+} and Fe^{2+}. It can be reasonably speculated that when La and Co substitute Sr hexaferrite simultaneously, Co^{2+} ions mainly occupy the $4f_1$ site since La-substitution causes Fe^{3+} to Fe^{2+} at the $2a$ site in La–Co SrM, which contributes to the enhancement of magnetocrystalline anisotropy [16]. It is quite interesting that different sites occupied by Co in various substitution cases lead to diverse magnetic properties.

From the perspective of temperature, the temperature dependence of H_A of all the Co-SrM samples along with SrM is shown in Fig. 5(b). The H_A of Co-SrM is larger than that of SrM for $0 < x \leq 0.11$ over the whole temperature range. It is known that the coercivity H_{cJ} is primarily dependent on magnetocrystalline anisotropy and structure parameters. Therefore, Co-SrM for $0.03 < x \leq 0.11$ has the potential to be used as permanent magnets. But for $0.11 < x \leq 0.15$, H_A begins to decline and drops sharply at $x = 0.31$. The decreased H_A of $Co_{0.31}$ is related to the type change of MA observed previously. At the same time, the H_A of Co-SrM is nearly independent of temperature similar to SrM, except $Co_{0.31}$. The H_A of $Co_{0.31}$ reduces significantly with decreasing temperature, and this temperature dependence was revealed in the neutron study of $Ba_{12-x}Co_xTi_xO_{19}$ (Co–Ti BaM), which maintained ferrimagnetic structure at 200–300 K when $x \leq 0.11$, but samples with $x \geq 0.8$ formed complex helimagnetic structure when temperature down to 2 K [47]. As a whole, Co^{2+} affects H_A in the full temperature range. Previous studies demonstrate that the effect of Fe^{2+} on MA is temperature localized, because the H_A of La-SrM exhibits disparate temperature dependence with various La concentrations [42], and the H_A of unequal substitution of La–Co SrM also largely depends on temperature [18]. It is considered to be the difference between spin-orbit interactions of Co^{2+} and Fe^{2+}, which is the origin of single-ion anisotropy. The value of λ/κ_B is reported to be approximately −256 and −148 K for Co^{2+} and Fe^{2+}, respectively [64], where λ is the spin-orbit coupling constant and κ_B is the Boltzmann constant, 1.38×10^{-16} erg/K. At high temperatures, the spin-orbit interaction of Fe^{2+} is likely to be highly suppressed by thermal fluctuation owing to the small λ but Co^{2+} doesn't.

4. Conclusion

The effects of Co-substitution on lattice parameters, Curie temperature, saturation magnetization, and uniaxial magnetocrystalline anisotropy (MA) were studied thoroughly through $SrFe_{12-x}Co_xO_{19}$ (Co-SrM) single crystals. First, due to the oxygen vacancy formed by charge compensation, the lattice parameters of Co-SrM increased briefly and then decreased monotonically. And since Co^{2+} tends to occupy the majority spin up sites of Co-SrM, the saturation magnetization M_S continued to decrease. Meanwhile, the MA of Co^{2+} single ion was discussed in detail from the perspective of concentration and temperature. Unlike Fe^{2+}, the effect of Co^{2+} on magnetic anisotropy field H_A was over the full temperature range. However, the enhancement H_A of Co-SrM for $0.03 < x \leq 0.11$ was observed for the first time, even higher than that of La–Co SrM, which is favorable for the application of permanent magnets. But for $x \geq 0.15$, the introduction of Co^{2+} preferred the planar MA, resulting in a significant loss of H_A in Co-SrM. The variations of MA can contribute to the formation of the nonlinear magnetic structure to induce electric polarization, thus the Co-SrM with high Co concentration can be used as magnetoelectric material. As Co single ion effect on MA revealed, the enhanced MA of La–Co SrM is more clarified. Since the occupation of spin-up $12k$ and $2a$ sites, the uniaxial anisotropy of Co-SrM was diluted. But the co-substitution with excess La^{3+} produces Fe^{2+} at the $2a$ site and makes Co^{2+} mainly occupy other spin-down sites, which clearly shows different effects of Co^{2+} on magnetocrystalline anisotropy in different cases.

CRediT authorship contribution statement

Ruoshui Liu: Conceptualization, Methodology, Investigation, Writing – original draft. Lichen Wang: Writing – review & editing. Xiang Yu: Formal analysis. Zhiyi Xu: Writing – review & editing. Huayang Gong: Supervision. Tongyun Zhao: Supervision. Fengxia Hu: Resources, Supervision. Baogen Shen: Resouces, Supervision.

Declaration of competing interest

The authors declare that they have no known competing financial interests or personal relationships that could have appeared to influence the work reported in this paper.

Acknowledgments

This work was supported by the Science Center of the National Science Foundation of China (52088101), the National Key Research and Development Program of China (2021YFB3501202, 2020YFA0711502, 2019YFA0704900, 2018YFA0305704), the National Natural Sciences Foundation of China (U1832219, 51971240, 52101228), the Strategic Priority Research Program B (XDB33030200) and the key program of the Chinese Academy of Sciences (ZDRW–CN–2021-3).

References

[1] R.C. Pullar, Hexagonal ferrites: a review of the synthesis, properties and applications of hexaferrite ceramics, Prog. Mater. Sci. 57 (2012) 1191–1334, https://doi.org/10.1016/j.pmatsci.2012.04.001.
[2] J.J. Went, G.W. Rathenau, E.W. Gorter, G.W.V. Oosterhout, Ferroxdure, a class of new permanent magnet materials, Philips Tech. Rev. 13 (1952) 194–208.
[3] C. Granados-Miralles, P. Jenuš, On the potential of hard ferrite ceramics for permanent magnet technology—a review on sintering strategies, J. Phys. Appl. Phys. 54 (2021) 303001, https://doi.org/10.1088/1361-6463/abfad4.
[4] C. de Julian Fernandez, C. Sangregorio, J. de la Figuera, B. Belec, D. Makovec, A. Quesada, Topical review: progress and prospects of hard hexaferrites for permanent magnet applications, J. Phys. Appl. Phys. 54 (2021) 153001, https://doi.org/10.1088/1361-6463/abd272.
[5] K. Iida, Y. Minachi, K. Masuzawa, M. Kawakami, H. Nishio, H. Taguchi, High - performance ferrite magnets: M - type Sr - ferrite containing lanthanum and cobalt, J. Magn. Soc. Jpn. 23 (1999) 1093–1096, https://doi.org/10.3379/jmsjmag.23.1093.
[6] Y. Ogata, Y. Kubota, T. Takami, M. Tokunaga, T. Shinokara, Improvements of magnetic properties of Sr ferrite magnets by substitutions of La and Co, IEEE Trans. Magn. 35 (1999) 3334–3336, https://doi.org/10.1109/20.800516.
[7] J.M. Le Breton, J. Teillet, G. Wiesinger, A. Morel, F. Kools, P. Tenaud, Mossbauer investigation of Sr-Fe-O hexaferrites with La-Co addition, IEEE Trans. Magn. 38 (2002) 2952–2954, https://doi.org/10.1109/tmag.2002.803177.
[8] A. Morel, J.M. Le Breton, J. Kreisel, G. Wiesinger, F. Kools, P. Tenaud, Sublattice occupation in Sr1−xLaxFe12−xCoxO19 hexagonal ferrite analyzed by Mössbauer spectrometry and Raman spectroscopy, J. Magn. Magn Mater. 242–245 (2002) 1405–1407, https://doi.org/10.1016/s0304-8853(01)00962-3.
[9] M.W. Pieper, F. Kools, A. Morel, NMR characterization of Co sites in La+Co-doped Sr hexaferrites with enhanced magnetic anisotropy, Phys. Rev. B 65 (2002), 184402, https://doi.org/10.1103/PhysRevB.65.184402.
[10] L. Lechevallier, J.M. Le Breton, J. Teillet, A. Morel, F. Kools, P. Tenaud, Mössbauer investigation of Sr1−xLaxFe12−yCoyO19 ferrites, Phys. B Condens. Matter 327 (2003) 135–139, https://doi.org/10.1016/s0921-4526(02)01712-x.
[11] D.H. Choi, S.W. Lee, I.-B. Shim, C.S. Kim, Mössbauer studies for La–Co substituted strontium ferrite, J. Magn. Magn Mater. 304 (2006) e243–e245, https://doi.org/10.1016/j.jmmm.2006.01.151.

[12] M. Oura, N. Nagasawa, S. Ikeda, A. Shimoda, T. Waki, Y. Tabata, H. Nakamura, N. Hiraoka, H. Kobayashi, 57Fe Mössbauer and Co K β x-ray emission spectroscopic investigations of La-Co and La substituted strontium hexaferrite, J. Appl. Phys. 123 (2018), 033907, https://doi.org/10.1063/1.5011244.
[13] H. Sakai, T. Hattori, Y. Tokunaga, S. Kambe, H. Ueda, Y. Tanioku, C. Michioka, K. Yoshimura, K. Takao, A. Shimoda, T. Waki, Y. Tabata, H. Nakamura, Occupation sites and valence states of Co dopants in (La, Co)-codoped M-type Sr ferrite: 57Fe and 59Co nuclear magnetic resonance studies, Phys. Rev. B 98 (2018), 064403, https://doi.org/10.1103/PhysRevB.98.064403.
[14] H. Nakamura, T. Waki, Y. Tabata, C. Mény, Co site preference and site-selective substitution in La–Co co-substituted magnetoplumbite-type strontium ferrites probed by 59Co nuclear magnetic resonance, J. Phys.: Materials 2 (2019), 015007, https://doi.org/10.1088/2515-7639/aaf540.
[15] S. Mahadevan, V. Sathe, V. Raghavendra Reddy, P. Sharma, Site occupation and magnetic studies in La–Co-substituted barium hexaferrite, IEEE Trans. Magn. 56 (2020) 1–6, https://doi.org/10.1109/tmag.2020.3014071.
[16] N. Nagasawa, M. Oura, S. Ikeda, T. Waki, Y. Tabata, H. Nakamura, H. Kobayashi, Magnetic anisotropies of La–Co substituted M-type Sr hexaferrites studied by 57Fe Mössbauer spectroscopy with external magnetic fields, J. Appl. Phys. 128 (2020), 133901, https://doi.org/10.1063/5.0019954.
[17] A. Shimoda, K. Takao, K. Uji, T. Waki, Y. Tabata, H. Nakamura, Flux growth of magnetoplumbite-type strontium ferrite single crystals with La–Co co-substitution, J. Solid State Chem. 239 (2016) 153–158, https://doi.org/10.1016/j.jssc.2016.04.031.
[18] H. Ueda, Y. Tanioku, C. Michioka, K. Yoshimura, Magnetocrystalline anisotropy of La- and Co-substituted M-type strontium ferrites: role of Co2+ and Fe2+, Phys. Rev. B 95 (2017) https://doi.org/10.1103/PhysRevB.95.224421.
[19] J. Lee, E.J. Lee, T.Y. Hwang, J. Kim, Y.H. Choa, Anisotropic characteristics and improved magnetic performance of Ca-La-Co-substituted strontium hexaferrite nanomagnets, Sci. Rep. 10 (2020), 15929, https://doi.org/10.1038/s41598-020-72608-0.
[20] T. Waki, K. Takao, Y. Tabata, H. Nakamura, Single crystal synthesis and magnetic properties of Co2+-substituted and non-substituted magnetoplumbite-type Na–La ferrite, J. Solid State Chem. 282 (2020), 121071, https://doi.org/10.1016/j.jssc.2019.121071.
[21] X.Z. Zhou, A.H. Morrish, Z. Yang, H.X. Zeng, Co-Sn substituted barium ferrite particles for perpendicular magnetic recording, J. Appl. Phys. 75 (1994) 5556–5558, https://doi.org/10.1063/1.355687.
[22] E.D. Solovyova, E.V. Pashkova, V.P. Ivanitski, O.I. V′yunov, A.G. Belous, Mössbauer and X-ray diffraction study of Co2+–Si4+ substituted M-type barium hexaferrite BaFe12−2xCoxSixO19±γ, J. Magn. Magn Mater. 330 (2013) 72–75, https://doi.org/10.1016/j.jmmm.2012.10.035.
[23] W. Zhang, Y. Bai, X. Han, L. Wang, X. Lu, L. Qiao, Magnetic properties of Co–Ti substituted barium hexaferrite, J. Alloys Compd. 546 (2013) 234–238, https://doi.org/10.1016/j.jallcom.2012.08.029.
[24] S.E. Shirsath, X. Liu, Y. Yasukawa, S. Li, A. Morisako, Switching of magnetic easy-axis using crystal orientation for large perpendicular coercivity in CoFe2O4 thin film, Sci. Rep. 6 (2016), https://doi.org/10.1038/srep30074.
[25] S.E. Shirsath, X. Liu, M.H.N. Assadi, A. Younis, Y. Yasukawa, S.K. Karan, J. Zhang, J. Kim, D. Wang, A. Morisako, Y. Yamauchi, S. Li, Au quantum dots engineered room temperature crystallization and magnetic anisotropy in CoFe2O4 thin films, Nanoscale Horizons 4 (2019) 434–444, https://doi.org/10.1039/C8NH00278A.
[26] S.E. Shirsath, D. Wang, J. Zhang, A. Morisako, S. Li, X. Liu, Single-Crystal-like textured growth of CoFe2O4 thin film on an amorphous substrate: a self-bilayer approach, ACS Applied Electronic Materials 2 (2020) 3650–3657, https://doi.org/10.1021/acsaelm.0c00716.
[27] H.B. Lee, S.H. Chun, K.W. Shin, B.-G. Jeon, Y.S. Chai, K.H. Kim, J. Schefer, H. Chang, S.-N. Yun, T.-Y. Joung, J.-H. Chung, Heliconical magnetic order and field-induced multiferroicity of the Co2Y-type hexaferrite Ba0.3Sr1.7Co2Fe12O22, Phys. Rev. B 86 (2012), https://doi.org/10.1103/PhysRevB.86.094435.
[28] M. Komabuchi, D. Urushihara, Y. Kimata, M. Okabe, T. Asaka, K. Fukuda, K. Nakano, K. Yamamoto, Influence of cobalt substitution on the magnetocrystalline anisotropy of X-type hexaferrites Sr2Co Fe30−O46, J. Magn. Magn Mater. 498 (2020), https://doi.org/10.1016/j.jmmm.2019.166115.
[29] M. Komabuchi, D. Urushihara, Y. Kimata, M. Okabe, T. Asaka, K. Fukuda, Multiaxial magnetocrystalline anisotropy in the X-type hexaferrite Sr2Co2Fe28O46 at low temperature, Phys. Rev. B 100 (2019), https://doi.org/10.1103/PhysRevB.100.094406.
[30] Y. Ebrahimi, A.A. Sabbagh Alvani, A.A. Sarabi, H. Sameie, R. Salimi, M. Sabbagh Alvani, S. Moosakhani, A comprehensive study on the magnetic properties of nanocrystalline SrCo0.2Fe11.8O19 ceramics synthesized via diverse routes, Ceram. Int. 38 (2012) 3885–3892, https://doi.org/10.1016/j.ceramint.2012.01.040.
[31] A.M. K, K.T. Selvi, M. Priya, Effect of Co and Sm substitutions on the magnetic interactions of M-type strontium hexaferrite nanoparticles, J. Supercond. Nov. Magnetism 33 (2019) 713–720, https://doi.org/10.1007/s10948-019-05227-0.
[32] K.K. Mallick, P. Shepherd, R.J. Green, Magnetic properties of cobalt substituted M-type barium hexaferrite prepared by co-precipitation, J. Magn. Magn Mater. 312 (2007) 418–429, https://doi.org/10.1016/j.jmmm.2006.11.130.
[33] E. Roohani, H. Arabi, R. Sarhaddi, S. Sudkhah, M-type strontium hexaferrite nanoparticles prepared by sol-gel auto-combustion method: the role of Co substitution in structural, morphological, and magnetic properties, J. Supercond. Nov. Magnetism 30 (2017) 1599–1608, https://doi.org/10.1007/s10948-016-3966-4.
[34] J. Chen, Y. Wang, Y. Liu, H. Wang, Q. Yin, Q. Liu, C. Wu, Y. Chen, Investigation of oriented Co3+ doped M-type hexaferrite Sr0.5Ba0.5Fe12−xCoxO19 for microwave application, J. Mater. Sci. Mater. Electron. 29 (2018) 14371–14377, https://doi.org/10.1007/s10854-018-9492-3.
[35] G.B. Teh, S. Nagalingam, D.A. Jefferson, Preparation and studies of Co(II) and Co (III)-substituted barium ferrite prepared by sol–gel method, Mater. Chem. Phys. 101 (2007) 158–162, https://doi.org/10.1016/j.matchemphys.2006.03.008.
[36] X. Wu, W. Chen, W. Wu, Y. Ning, S. Chen, Synthesis of hexagonal Co3+-substituted Sr-ferrites via ball-milling assisted ceramic process and their magnetic properties, J. Mater. Sci. Mater. Electron. 28 (2017) 18815–18824, https://doi.org/10.1007/s10854-017-7831-4.
[37] M.Z. Shoushtari, S.E.M. Ghahfarokhi, F. Ranjbar, Synthesis and magnetic properties of SrFe12-xCoxO19 (x= 0- 2) hexaferrite nanoparticles, Adv. Mater. Res. 622–623 (2012) 925–929. https://doi.org/10.4028/www.scientific.net/AMR.622-623.925.
[38] T. Xie, L. Xu, C. Liu, Synthesis and properties of composite magnetic material SrCoxFe12-xO19 (x=0–0.3), Powder Technol. 232 (2012) 87–92, https://doi.org/10.1016/j.powtec.2012.08.015.
[39] D.A. Vinnik, D.A. Zherebtsov, L.S. Mashkovtseva, S. Nemrava, A.S. Semisalova, D. M. Galimov, S.A. Gudkova, I.V. Chumanov, L.I. Isaenko, R. Niewa, Growth, structural and magnetic characterization of Co- and Ni-substituted barium hexaferrite single crystals, J. Alloys Compd. 628 (2015) 480–484, https://doi.org/10.1016/j.jallcom.2014.12.124.
[40] J. Dho, E.K. Lee, J.Y. Park, N.H. Hur, Effects of the grain boundary on the coercivity of barium ferrite BaFe12O19, J. Magn. Magn Mater. 285 (2005) 164–168, https://doi.org/10.1016/j.jmmm.2004.07.033.
[41] V. Dixit, S.-G. Kim, J. Park, Y.-K. Hong, Effect of ionic substitutions on the magnetic properties of strontium hexaferrite: a first principles study, AIP Adv. 7 (2017), 115209, https://doi.org/10.1063/1.4995309.
[42] M. Küpferling, R. Grössinger, M.W. Pieper, G. Wiesinger, H. Michor, C. Ritter, F. Kubel, Structural phase transition and magnetic anisotropy of La-substitutedM-type Sr hexaferrite, Phys. Rev. B 73 (2006), 144408, https://doi.org/10.1103/PhysRevB.73.144408.
[43] A. Aharoni, Demagnetizing factors for rectangular ferromagnetic prisms, J. Appl. Phys. 83 (1998) 3432–3434, https://doi.org/10.1063/1.367113.
[44] G. Asti, S. Rinaldi, Nonanaliticity of the magnetization curve: application to the measurement of anisotropy in polycrystalline samples, Phys. Rev. Lett. 28 (1972) 1584–1586, https://doi.org/10.1103/PhysRevLett.28.1584.
[45] P.G. Bercoff, C. Herme, S.E. Jacobo, The influence of Nd–Co substitution on the magnetic properties of non-stoichiometric strontium hexaferrite nanoparticles, J. Magn. Magn Mater. 321 (2009) 2245–2250, https://doi.org/10.1016/j.jmmm.2009.01.033.
[46] A.M. Balbashov, M.E. Voronchikhina, A.A. Mukhin, V.Y. Ivanov, L.D. Iskhakova, Floating zone crystal growth and magnetic properties of M-type Co-substituted strontium hexaferrites, J. Cryst. Growth 524 (2019), 125158, https://doi.org/10.1016/j.jcrysgro.2019.125158.
[47] J. Kreisel, H. Vincent, F. Tasset, M. Paté, J.P. Ganne, An investigation of the magnetic anisotropy change in BaFe12−2xTixCoxO19 single crystals, J. Magn. Magn Mater. 224 (2001) 17–29, https://doi.org/10.1016/s0304-8853(00)01355-x.
[48] M. Robbins, E. Banks, Effect of fluoride-compensated Co2+on the anisotropy of BaFe12O19, J. Appl. Phys. 34 (1963) 1260–1261, https://doi.org/10.1063/1.1729461.
[49] M. Zhang, Q. Liu, G. Zhu, S. Xu, Magnetic properties of Co and Ti co-doped strontium hexaferrite prepared by sol–gel method, Appl. Phys. A 125 (2019) 191, https://doi.org/10.1007/s00339-019-2500-5.
[50] W. Zhang, Q. Zhu, R. Tang, H. Zhou, J. Zhang, J. Jiang, H. Yang, X. Su, Temperature dependent magnetic properties of conical magnetic structure M-type hexaferrites BaFe10.2Sc1.8O19 and SrFe10.2Sc1.8O19, J. Alloys Compd. 750 (2018) 368–374, https://doi.org/10.1016/j.jallcom.2018.03.260.
[51] C. Jianfeng, L. Yingli, Y. Qisheng, Computational and experimental study on cation distribution of Cobalt substituted barium hexaferrites BaFe12−xCoxO19 (x = 0, 0.3, 0.6, 0.9) for circulator applications, J. Alloys Compd. 891 (2022), 161917, https://doi.org/10.1016/j.jallcom.2021.161917.
[52] S. Singhal, K. Kaur, S. Jauhar, S. Bhukal, S. Bansal, Structural and magnetic properties of $BaCo_xFe_{12x}O_{19}$ (x = 0.2, 0.4, 0.6, & 1.0) nanoferrites synthesized via citrate sol-gel method, World J. Condens. Matter Phys. (2011) 101–104, https://doi.org/10.4236/wjcmp.2011.13016, 01.
[53] D.V. Ruikar, P. Kashid, S. Supugade, N. Pisal, V. Puri, Structural, electrical and magnetic properties of SrCoxFe12− xO19 (0≤ x≤ 1) prepared by co-precipitation method, Advances in Ceramic Science and Engineering 2 (2013) 72–77.
[54] Y. Xu, G.-L. Yang, D.-P. Chu, H.-R. Zhai, Theory of the single ion magnetocrystalline anisotropy of 3d ions, Phys. Status Solidi 157 (1990) 685–693, https://doi.org/10.1002/pssb.2221570221.
[55] J. Inoue, H. Onoda, H. Yanagihara, Uniaxial magnetic anisotropy of transition metal oxides: role of local lattice deformation, J. Phys. Appl. Phys. 53 (2020), 195003, https://doi.org/10.1088/1361-6463/ab7324.
[56] T. Waki, K. Uji, Y. Tabata, H. Nakamura, Single-crystal growth and magnetic properties of Co-substituted Ca–La magnetoplumbite-type ferrite, J. Solid State Chem. 270 (2019) 366–369, https://doi.org/10.1016/j.jssc.2018.11.036.
[57] E. Brando, H. Vincent, O. Dubrinfaut, A. Fourrier-Lamer, R. Lebourgeois, Microwave electromagnetic characteristics of new substituted M-hexaferrites BaFe12-2xAxMexO19 (A= Ru, Ir; Me= Co, Zn), C1, J. Phys. IV 7 (1997) 421–422. C421.
[58] H.-S. Cho, S.-S. Kim, M-hexaferrites with planar magnetic anisotropy and their application to high-frequency microwave absorbers, IEEE Trans. Magn. 35 (1999) 3151–3153.

[59] H. Vincent, B. Sugg, V. Lefez, B. Bochu, D. Boursier, P. Chaudouet, Crystal growth, X-ray and magnetic studies of planar anisotropy M-hexaferrites BaFe12-2xIrxMexO19 (Me= Zn, Co), J. Magn. Magn Mater. 101 (1991) 170–172.
[60] H. Vincent, E. Brando, B. Sugg, Cationic distribution in relation to the magnetic properties of new M-hexaferrites with planar magnetic anisotropy BaFe12-2xIrxMexO19 (Me= Co, Zn, x≈ 0.85 and x≈ 0.50), J. Solid State Chem. 120 (1995) 17–22.
[61] L. Lechevallier, J.M. Le Breton, A. Morel, P. Tenaud, Influence of the presence of Co on the rare earth solubility in M-type hexaferrite powders, J. Magn. Magn Mater. 316 (2007) e109–e111, https://doi.org/10.1016/j.jmmm.2007.02.042.
[62] D. Seifert, J. Töpfer, M. Stadelbauer, R. Grössinger, J.-M. Le Breton, Rare-earth-substituted Sr1−xLnxFe12O19 hexagonal ferrites, J. Am. Ceram. Soc. 94 (2011) 2109–2118, https://doi.org/10.1111/j.1551-2916.2010.04363.x.
[63] M. Küpferling, P. Novák, K. Knížek, M.W. Pieper, R. Grössinger, G. Wiesinger, M. Reissner, Magnetism in La substituted Sr hexaferrite, J. Appl. Phys. 97 (2005), https://doi.org/10.1063/1.1855710.
[64] D. Alders, R. Coehoorn, W.J.M. de Jonge, Single-ion anisotropy of localized-electron compounds, Phys. Rev. B 63 (2001), 054407, https://doi.org/10.1103/PhysRevB.63.054407.